Few-subcarrier QPSK-OFDM wireless Ka-band delivery with pre-coding-assisted frequency doubling

Wen Zhou[1,2*], Jianjun Yu[1], Li Zhao[1,2], Kaihui Wang[1], Miao Kong[1], Jiao Zhang[1], You-Wei Chen[2], Shuyi Shen[2] and Gee-Kung Chang[2]

1) Shanghai Institute for Advanced Communication and Data Science, Fudan University, Shanghai 20043, China
2) School of Electrical and Computer Engineering, Georgia Institute of Technology, Atlanta, GA, 30308, USA (*zwen@fudan.edu.cn)

Abstract: We experimentally demonstrated a Ka-band dual/four-subcarrier QPSK-OFDM delivery over 25-km SMF and 1-m wireless link. To our knowledge, this is the first time to achieve few-subcarrier QPSK-OFDM signal generation and wireless transmission using pre-coding technique.

OCIS codes: (060.0060) Fiber optics and optical communications; (060.5625) Radio frequency photonics.

1. Introduction

The continuously increased growth of mobile data and end user number creates some challenges in the future 5G wireless broadband network, e.g., supporting high data rate and high mobility for user equipment. In order to address those issues, advanced modulation format with high spectrum efficiency becomes an effective solution. 3GPP 38.101 standard focuses on orthogonal frequency-division multiplexing (OFDM) modulation scheme, which provides excellent spectrum efficiency and can be compatible with present 4G networks. The traditional OFDM utilizes the cyclic prefix, which increase the overhead of the transmitted data stream and thus reduces the system throughput [1]. Unfortunately, higher peak-to-average power ratio (PAPR) value induced by larger FFT/IFFT size is still a critical problem, which causes higher nonlinear effects and thus limits the transmission fiber distance, especially when the input launched power is very high. Compared with the proposed PAPR reduction measures [2-3], the most direct and effective method is to shorten the number of OFDM subcarriers [4]. Meanwhile, Ka-band (28-39GHz) is considered as a prime candidate for satisfying 5G capacity demands of tens of gigabits per second, and it has a small atmosphere loss below 0.07dB/km. In 2015, the pre-coding mm-wave generation technique was proposed in the traditional OFDM system [5-6], which employed a bind algorithm to realize the pre-coding of lots of IFFT subcarriers. Considering both PAPR problem and the algorithm complexity, few-subcarrier OFDM signal generation and wireless transmission at Ka-band range are interesting to be explored and investigated.

In this paper, we experimentally demonstrated a Ka-band few-subcarrier QPSK-OFDM signal generation and wireless transmission based on a single-driven MZM. At the transmitter, a few-subcarrier QPSK-OFDM signal after the inverse fast Fourier transform (IFFT) operation would transfer to a higher modulation format in the time domain, which is pre-coded and then up-converted into a radio frequency (RF) *fs* for driving the employed MZM. The MZM is DC-biased at the minimum transmission point to realize two symmetric first-order subcarriers generation. The generated two subcarriers are heterodyne beating by the single-ended photodiode (PD) to generate the desired QPSK-OFDM signal at 2*fs*. We discussed dual-subcarrier and four-subcarrier QPSK-OFDM generation, respectively. The experimental results show that up to 4-Gbaud QPSK-OFDM signal with NFFT =2, 4 at 30-GHz can be transmitted over 25-km SMF and 1-m wireless distance with a bit-error-ratio (BER) less than 3.8×10^{-3}. To the best of our knowledge, this is the first time to achieve a Ka-band few-subcarrier QPSK-OFDM signal generation and wireless transmission using the pre-coding technique.

2. Few-subcarrier OFDM pre-coding principle

Figure 1(a) specifies the Ka-band QPSK-OFDM mm-wave vector signal generation process employing pre-coding frequency doubling technique. With the aid of MATLAB software, a pseudo-random binary sequence (PRBS) is firstly mapped to QPSK signal as shown in Fig. 1(b1), and then serial-to-parallel (S/P) converted and IFFT transformed into 9-QAM with two effective subcarriers (NFFT=2) as shown in Fig. 1. (c1). Next, Figs. 1(d1)-1(e1) give 9-QAM constellation distributions after amplitude and phase pre-coding, respectively. Finally, the QPSK-OFDM data stream at *fs* can be produced after the parallel-to-serial (P/S) and frequency up-conversion. After a high-speed digital-to-analog converter (DAC), the analog electrical QPSK-OFDM signal is used to drive the applied MZM. Inset (i) shows that the output power of the deployed MZM varies with the DC-bias. Through controlling the DC-bias, MZM works at its minimum transmission power point to achieve optical OFDM carrier suppression (OCS) modulation. Different from the dual-carrier generation, IFFT four-carrier (NFFT=4) signal changes to 25-QAM with 6 reference circles as shown in Fig.1 (c2). So more amplitude levels should be pre-coded than 9-QAM as shown in Fig. 1(d2)-(e2).
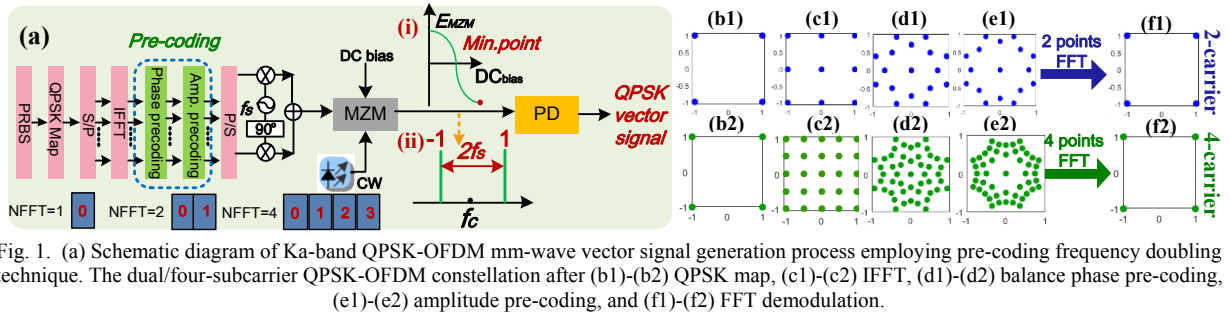
Fig. 1. (a) Schematic diagram of Ka-band QPSK-OFDM mm-wave vector signal generation process employing pre-coding frequency doubling technique. The dual/four-subcarrier QPSK-OFDM constellation after (b1)-(b2) QPSK map, (c1)-(c2) IFFT, (d1)-(d2) balance phase pre-coding, (e1)-(e2) amplitude pre-coding, and (f1)-(f2) FFT demodulation.

Based on the balanced pre-coding scheme, the phase $\varphi_k(t)$ of driving IFFT signal should satisfy $\varphi_k(t) = \dfrac{\varphi_{regular\_k} + 2m\pi}{2}$ ($m = 0,1$) as shown in Fig. 1(d1) and (d2), which can effectively improve the receiver sensitivity [7]. Considering both 2- and 4-subcarrier OFDM cases, the normalized amplitude of 9-QAM with 3 reference circles is derived as 0, 0.83 and 1, and that of 25-QAM with 6 reference circles can be pre-coded as 0, 0.594, 0.704, 0.84, 0.891 and 1. The pre-coded OFDM signal can be finally received and digitally processed by serial-to-parallel (S/P) and FFT demodulation steps, and the recovered QPSK constellation for dual- and four-carrier OFDM signals can be obtained in Fig. 1(f1) and (f2), respectively.
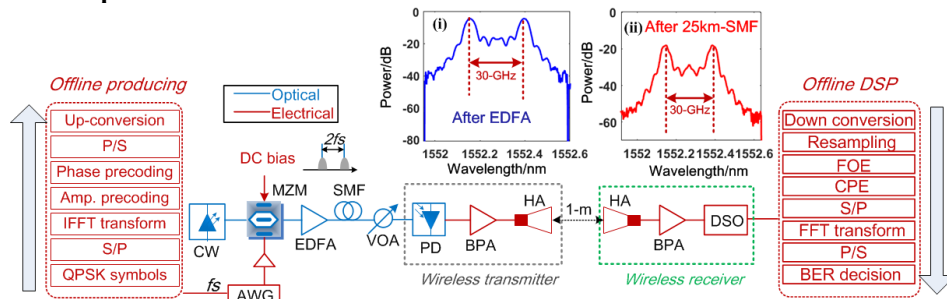
3. Experimental setup

Fig. 2. The experimental setup for the Ka-band QPSK-OFDM after 25-km SMF and 9-m wireless transmission based on a single MZM.

Figure 2 shows the photonics-aided Ka-band QPSK-OFDM over 25-km SMF and 9-m wireless transmission experimental setup based on a single MZM. As indicated in the OFDM signal offline producing steps in the red block, the QPSK-mapping symbols with a length of 2^{13}-1 are firstly S/P converted and then IFFT transformed. After amplitude (Amp.) and phase pre-coding, the OFDM pre-coded signals are subsequently P/S and up-converted into RF data streams. This RF signal at fs is digital-to-analog converted by a commercial 80GSa/s AWG and then amplified by a cascaded electrical amplifier (EA), which can be used to drive the MZM. The employed MZM with a 3dB optical bandwidth of 30GHz, half-wave voltage of 4.6 V at 1 GHz and 5-dB insertion loss is biased at 2.5 V and operated at its minimum transmission point. The lightwave are generated at 1552.25-nm center wavelength with line-width of 100-kHz and average output power of 16 dBm from the external cavity laser (ECL) with full C-band operating range. Based on OCS operation, the CW modulated by MZM has two ±1st-order subcarriers with frequency space of $2fs$ and 5 Gbaud QPSK-OFDM signal. Here, we use a PM-EDFA before 25km-SMF transmission to amplify the optical power, and the corresponding optical spectrum is depicted in Fig. 2(i) when fs is set as 15 GHz. As shown in Fig. 2(ii), the two 30-GHz spaced tones have different transmission speed due to the fiber dispersion, which will result in large power penalty and pulse broadening caused by the fading effect and bit walk-off effect. In order to avoid the saturation effect, we also adopt a VOA to adjust the power into the single-ended 50 GHz PD. Thus, mm-wave at $2fs$ can be generated after heterodyne beating in PD. Before wireless transmission, the generated mm-wave signal can be is boosted via the band-pass amplifier (BPA) with 35-dB gain at DC-50 GHz band. In the wireless transmission link, the mm-wave signal is transmitted and received over 1-m air space distance by a pair horn antennas (HAs) operating from 26 GHz to 40 GHz with 25 dBi gain. At the receiver-side, the same BPA as the one at Tx-side is employed to amplify the received signal from HA. Finally, the boosted signal can be captured by the real time digital oscillator (OSC) with a sampling rate of 120 GSa/s and electrical bandwidth of 45 GHz, and recovered by the following digital signal processing (DSP) including down conversion, resampling, frequency offset estimation (FOE), carrier phase recovery (CPR), S/P conversion, FFT demodulation, P/S and BER decision.

4. Experimental results for Ka-band few-carrier QPSK-OFDM signal wireless transmission

Figure 3(a) gives the BER measured results for both 5 Gbaud 30 GHz dual- and four-subcarrier QPSK-OFDM reception with different input power into PD. We can see that BER performance improves with the increasing received optical power, and it achieves as low as 10^{-4} when the input received power is -0.5dBm. Furthermore, dual-carrier OFDM signal performs better than the four-carrier when the power into PD is low. But, it is contrary in the higher received power region. For lower SNR, high-order QAM is very sensitive to noise interference and channel distortion. So 25-QAM is more affected than 9-QAM and the QPSK signal after dual-carrier IFFT transformation gets a better performance. In contrast, BER of four-carrier signal is lower than dual-carrier with higher SNR.
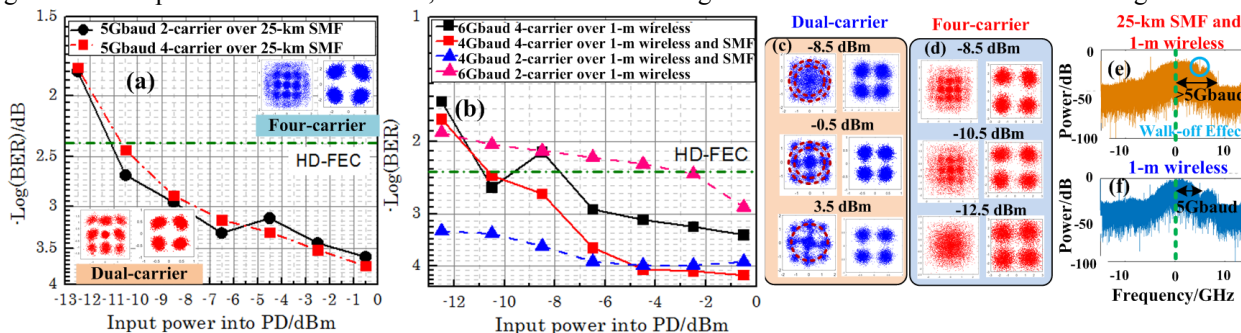

Fig. 3. (a) BER performances vs. input power into PD when 5Gbaud dual- and four-carrier QPSK-OFDM signals are transmitted over 25-km SMF. (b) BER performances vs. the optical power into PD for dual-, and four-subcarrier QPSK-OFDM delivery over 25-km SMF and 1-m wireless link, respectively, the recovered QPSK constellation diagram of (c) 2-carrier,(d) 4-carrier, (e)-(f) the down-converted spectrum.

We also discuss BER results versus the input power into PD when 2- and 4-subcarrier QPSK-OFDM signal is transmitted over 25-km fiber link and 1-m free space distance in Fig. 3(b), which depicts that the performance can be enhanced obviously with high SNR. Figs. 3(c) and (d) show that the recovered QPSK diagrams of 6 Gbaud dual- and four-carrier QPSK-OFDM signal are clearer with the increasing input power. However, the saturation effect of PD would result in BER performance degradation with a larger optical power. It can be found that 9-QAM constellation distribution has been compressed into a reference circle when the optical power grows to 3.5 dBm in Fig. 3(c). Note that the dispersion-induced walk-off effect (WOE) $\tau = D \times L \times \Delta\lambda$, which is the limiting factor of the fiber transmission speed [8]. Compared with Fig. 3(e) and (f), the baseband bandwidth of 5-Gbaud 2-carrier QPSK-OFDM signal is extended to above 5-Gbaud after 25-km SMF and 1-m wireless transmission, which is induced by WOE. Unfortunately, the performance would be further degraded due to HA band-pass filtering effect, as the blue circle shown in Fig. 3(e). Both from the analysis of dual- and four-subcarrier OFDM SMF and wireless transmission, it can be concluded that 2-subcarrier OFDM has a better performance than 4-subcarrier when the signal power is low. It is because smaller distance between 25-QAM constellation points lessen anti-interference ability of receiving system sharply compared with low order 9-QAM format. On the contrary, with a relatively large SNR, channel estimation is more precise for 4-subcarrier OFDM rather than 2-subcarrier case.

4. Conclusions

Different with the blind pre-coding method employed for traditional OFDM with a great number of subcarriers, an accurate and simple pre-coding model of few-carrier OFDM vector signal generation is proposed in this paper, which also effectively avoids the higher PAPR induced nonlinear problem. We experimentally demonstrated a 12Gbit/s 30-GHz 1-m wireless transmission employing a single MZM biased at its OCS operation voltage, and an 8Gbit/s dual- and four-subcarrier QPSK-OFDM signal delivery over 25-km SMF and 1-m wireless link.

5. References

[1] W. Shieh and I. Djordjevic, OFDM for Optical Communications (Academic, 2010).
[2] C. Li, Q. Yang, T. Jiang, Z. He, M. Luo, C. Li, X. Xiao, D. Xue, and X. Yi, "Investigation of coherent optical multiband DFT-S OFDM in long haul transmission," IEEE Photon. Technol. Lett. **24**, 1704-1707 (2012).
[3] H. Wang, Y. Li, X. Yi, et al. "APSK modulated CO-OFDM system with increased tolerance toward fiber nonlinearity," IEEE Photon. Technol. Lett. **24**, 1085-1087 (2012).
[4] F. Li, J. Zhang, J. Yu. "Blind equalization for dual-polarization two-subcarrier coherent QPSK-OFDM signals," Opt. Letters, **39**, 201 (2014).
[5] J. Xiao, X. Li, Y. Xu, et al. "W-band OFDM photonic vector signal generation employing a single Mach-Zehnder modulator and precoding," Opt. Express, **23**, 24029 (2015).
[6] J. Xiao, Z. Zhang, X. Li. "OFDM vector signal generation based on optical carrier suppression," IEEE Photon. Technol. Lett. **27**, 1-1 (2015).
[7] Y. Wang, Y. Xu, X. Li, J. Yu, and N. Chi, "Balanced precoding technique for vector signal generation based on OCS," IEEE Photon. Technol. Lett. **27**, 2469-2472 (2015).
[8] J. Ma, J. Yu, C. Yu, X. Xin, J. Zeng, and L. Chen, "Fiber dispersion influence on transmission of the optical millimeter-waves generated using LN-MZM intensity modulation," J. Lightw. Technol., **25**, 3244–3256 (2007).